JOC*Article*

Azobenzene Derivatives Carrying a Nitroxide Radical

Shin'ichi Nakatsuji,*,† Masahiro Fujino,† Satoko Hasegawa,† Hiroki Akutsu,† Jun-ichi Yamada,† Vladimir S. Gurman,‡ and Andrey Kh.Vorobiev*,‡

Department of Material Science, Graduate School of Material Science, University of Hyogo, 3-2-1 Kouto, Kamigori, Hyogo 678-1297, Japan, and Department of Chemistry, Moscow State University, Leninskie Gory, Moscow 119992, Russia

nakatuji@sci.u-hyogo.ac.jp; vorobiev@excite.chem.msu.ru

Received November 2, 2006

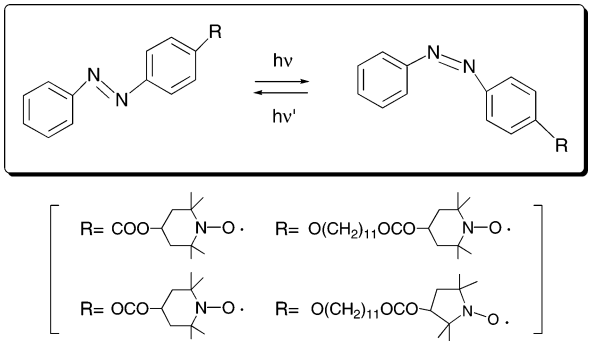

Several *trans*-azobenzene derivatives carrying a nitroxide (aminoxyl) radical (**2a**, **6a**−**12a**) were prepared, and their photoisomerization reactions to the corresponding *cis*-isomers were investigated. Although no fruitful results could be obtained for the photoisomerizations of the derivatives with *para*-subsituents (**9a**−**12a**), the unsubstututed derivatives at the *para*-position (**2a**, **6a**, **7a**, **8a**) were found to show photoisomerizations by irradiation to give the corresponding *cis*-isomers (**2b**, **6b**, **7b**, **8b**), being isolated as relatively stable solid materials, and the change of the intermolecular magnetic interactions was apparently observed by the structural change for each photochromic couple.

Introduction

There is a continuing trend in the field of molecular-based magnetic materials to develop multifunctional spin systems,[1] and the exploitation of organic photofunctional materials has attracted in this context much attention in recent years.[2] As a precedent example, Iwamura and his collaborators prepared a *trans*-azobenzene derivative carrying two nitronyl nitroxide groups and reported it to show UV as well as EPR spectral change upon irradiation in solution.[3] Since then, a variety of organic and organometallic photofunctional spin systems have been reported until now, and they include several impressive examples of diarylethene derivatives,[4] spin systems with a ferrocene moiety,[5] or metal complexes with a spiropyran photochromic unit.[6] In the course of our studies to develop novel organomagnetic materials, we have been interested in preparing multifunctional spin systems with conductivity, photofunctionality, or a liquid crystalline property by using stable radicals, especially nitroxide radicals, as spin sources. As for the spin systems with photofunctionality, we have so far proposed several photoresponsive spin systems by using such photochromic systems as norbornadiene/quadricyclane, spiropyran/merocyanine, anthracene/dimer, or naphthopyran/merocyanine. Azoben-

† University of Hyogo.
‡ Moscow State University.

(1) For recent reviews on molecular-based magnetic materials, see: (a) *Magnetic Properties of Organic Materials*; Lahti, P. M., Ed.; Marcel Dekker, Inc.: New York, Basel, 1999. (b) *Molecular Magnetism*; Itoh, K., Kinoshita, M., Eds.; Kodansha/Gordon and Breach Science Publishers: Tokyo, 2000. (c) *Structure and Bonding, Vol. 100, π-Electron Magnetism: From Molecule to Magnetic Materials*; Veciana, J., Ed.; Springer-Verlag: Berlin, 2001. (d) *Magnetism: Molecules to Materials*; Miller, J. S., Drillon, M., Eds.; Wiley-VCH: Weinheim, Germany, 2001−2005; Vols. I−V.

(2) Cf. Natatsuji, S. *Chem. Soc. Rev.* **2004**, *33*, 348.

(3) Hamachi, K; Matsuda, K.; Itoh, T.; Iwamura, H. *Bull. Chem. Soc. Jpn.* **1998**, *71*, 2937.

(4) Cf. Matsuda, K.; Irie, M. *J. Photochem. Photobiol., C* **2004**, *5*, 169 and references therein.

(5) (a) Ratera, I.; Ruiz-Molina, D.; Vidal-Gancedo, J.; Wurst, K.; Daro, N.; Létard, J.-F.; Rivira, C.; Veciana, J. *Angew. Chem., Int. Ed.* **2001**, *40*, 919. (b) Ratera, I.; Ruiz-Molina, D.; Vidal-Gancedo, J.; Novoa, J. J.; Wurst, K.; Létard, J.-F.; Rivira, C.; Veciana, J. *Chem.—Eur. J.* **2004**, *10*, 603.

(6) Bênard, S.; Riviere, E.; Yu, P.; Nakatani, K.; Delouis, J. F. *Chem. Mater.* **2001**, *13*, 159.

10.1021/jo062266f CCC: $37.00 © 2007 American Chemical Society
Published on Web 02/20/2007

CHART 1

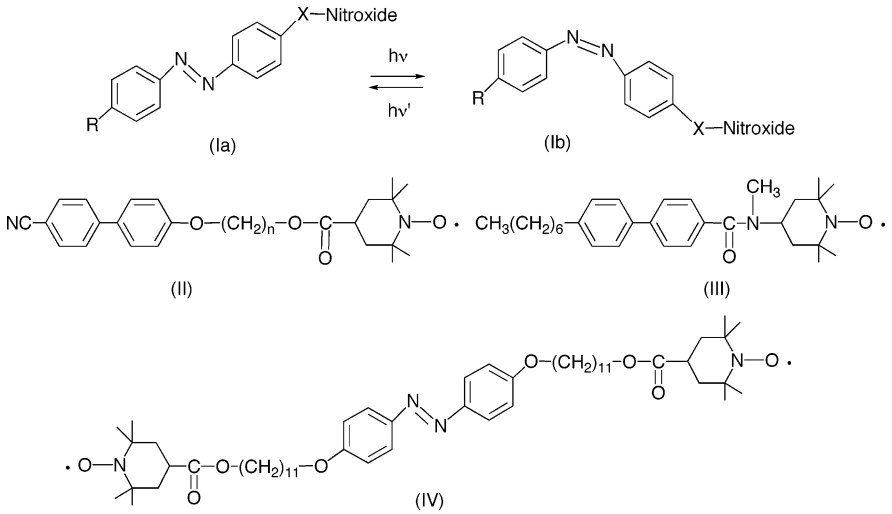

SCHEME 1

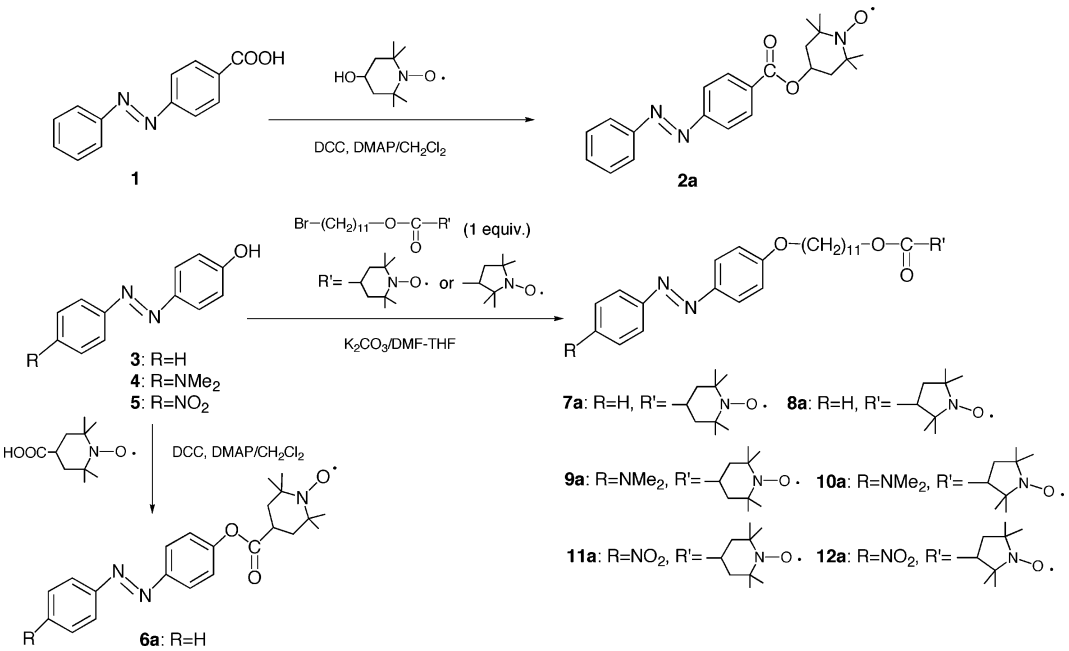

zene derivatives with stable radicals have also been attractive candidates for photofunctional spin systems, and even if there was initial apprehension of difficulty for the isolation of *cis*-isomers of azobenzene derivatives as inferred in another case,[3] we took the plunge to prepare some targeted compounds of the derivatives **I** (Chart 1). Among them, azobenzene derivatives carrying nitroxide radicals as well as long alkyl groups have particularly been focused upon, since the introduction of long alkyl groups is supposed to add a possible heat-responsive property as previously shown for compounds **II**[7] to inherent photofunctionality expected from the existence of an azobenzene core. It was anticipated through earlier studies that the specific assemblies of such molecules as **II** or **III**[8] with supramolecular structures might be relevant to the formation of the mesogenic phase and/or unusual thermomagnetic properties. Although no fruitful photoresponsive property could be realized in the biradical compound **IV** with an azobenzene moiety as well as long alkyl groups, probably because of the unstable nature of the corresponding *cis*-isomer, fairly large intermolecular magnetic interaction has been observed in the compound due mainly to its specific assembly structure in the solid state.[9] On the other hand, some *cis*-azobenzenes with a nitroxide group have been found to be isolable in the solid state, exhibiting differences in their magnetic properties compared with the corresponding *trans*-isomers. We herein describe the details of the preparation of such azobenzene derivatives carrying a nitroxide group that show photoresponsive properties together with the differences in their magnetic properties derived from the structural differences.[10]

Results and Discussion

Preparation of *trans*-Azobenzene Derivatives with a Nitroxide Group. The preparation of *trans*-azobenzene derivatives

(7) Nakatsuji, S.: Ikemoto, H.; Akutsu, H.; Yamada, J.; Mori, A. *J. Org. Chem.* **2003**, *68*, 1708.

(8) Nakatsuji, S.:Mizumoto, M.; Ikemoto, H.; Akutsu, H.; Yamada J. *Eur. J. Org. Chem.* **2002**, 1869.

(9) (a) Amano, T.; Akutsu, H.; Yamada, J.; Nakatsuji, S. *Chem. Lett.* **2004**, *33*, 382. (b)Nakatsuji, S.; Amano, T.; Akutsu, H.; Yamada, J. *J. Phys. Org. Chem.* **2006**, *19*, 333.

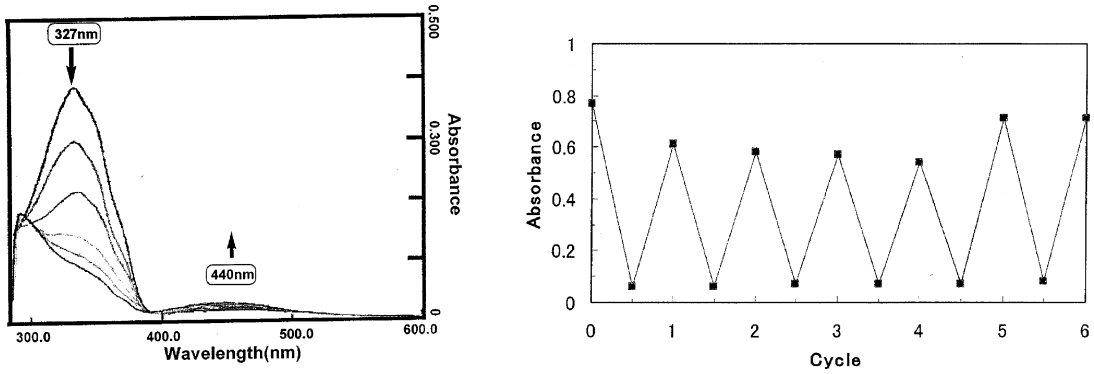

FIGURE 1. (Left) Time dependence of the absorption spectra for *trans*-isomer **2a** to *cis*-isomer **2b** every 5 min from the original absorption in dichloromethane. (Right) Change in the absorbance of the forward and backward reactions of the photoisomer couple **2a**/**2b** at 327 nm.

SCHEME 2

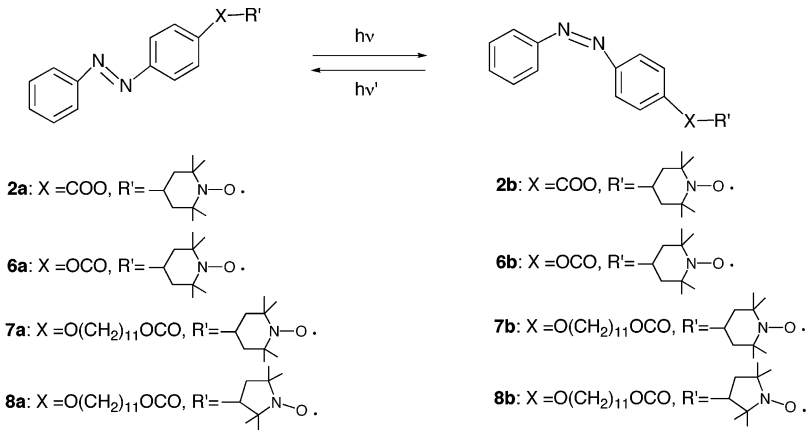

with a nitroxide group (**2a**, **6a**−**12a**) was carried out as shown in Scheme 1. A TEMPO (2,2,6,6-tetramethyl-1-piperidinyloxy)-substituted ester derivative (**2a**) was prepared in 66% yield by the condensation of 4-carboxyazobenzene (**1**) with 4-hydroxy-TEMPO using DCC and DMAP as the condensing reagents. Similarly, an isomeric ester (**6**) was obtained by using 4-hydroxyazobenzene (**3**) and 4-carboxyl-TEMPO in 74% yield. The treatment of **3** with (bromoundecanoxy)carbonyl-TEMPO[9] or the PROXYL (2,2,5,5-tetramethyl-1-pyrrolidinyloxy) derivative[9] gave the corresponding azobenzene derivatives with a TEMPO (**7a**) or PROXYL (**8a**) substituent in 72% and 71% yield, respectively. A couple of azobenzenes with *p*-dimethylamino or *p*-nitro substituents and with a TEMPO or PROXYL group (**9a**−**12a**) could similarly be prepared from the corresponding hydroxyazobenzenes **4** and **5**, although the yields were relatively low (**9a**, 16%; **10a**, 41%; **11a**, 30%; **12a**, 68%). The thermotropic properties of a series of azobenzenes thus prepared were examined by DSC measurements, but the endothermic peaks of their melting points could only be discerned for all of the compounds even those with a long alkoxy chain, indicating the absence of any liquid crystalline phase in the radicals.

Investigation of Photochemical Isomerizations of Azobenzene Derivatives with a Nitroxide. When *trans*-azobenzene with a TEMPO substituent (**2a**) was irradiated in dichloromethane solution with light of 365 nm, the absorption maxima at around 327 nm were found to decrease gradually while a new broad absorption at around 440 nm with an isosbestic point at 390 nm was developed in turn, indicating occurrence of photoisomerization in the solution (Figure 1, left). In spite of the initial apprehension and the fruitless experience for the photoisomerization of biradical compound **IV**,[9] the corresponding *cis*-isomer **2a** could fortunately be isolated after purification by short-column chromatography on SiO_2 as a relatively stable solid substance when kept in the dark and stored in a refrigerator. In turn, the backward reaction took place simply by the exposure of the powdery solid or a solution of the *cis*-isomer **2a** to diffused light or by illumination with a fluorescent lamp at ambient temperature for several hours, and hence, a reversible system could be constructed in principle in this case (Scheme 2). The forward and backward reactions could be repeated several times without appreciable decay (Figure 1, right) for the isomer couple **2a** and **2b**. The photoisomerization of the ester isomer **6a** proceeded quite similarly (cf. SI-1, Figure A; SI = Supporting Information), and the corresponding *cis*-isomer **6b** could also be isolated as a relatively stable solid. Even the azobenzenes with a long alkyl group and a TEMPO or a PROXYL group (**7a** or **8a**) were also found to occur by a similar irradiation to give the corresponding *cis*-isomers **7b** and **8b** as relatively stable solids,[10] while irradiation on the *para*-substituted derivatives **9a**−**12a** under various conditions resulted in photobleaching and/or recovery of the starting materials in solution, and hence, the isolation of the corresponding *cis*-isomers was unsuccessful so far as examined in these cases.

(10) Portions of this work have appeared as preliminary communications: (a) Fujino, M.; Amano, T.; Akutsu, H.; Yamada, J.; Nakatsuji, S. *Chem. Commun.* **2004**, 2310. (b) Amano, T.; Fujino, M.; Akutsu, H.; Yamada, J.; Nakatsuji, S. *Polyhedron* **2005**, *24*, 2614.

TABLE 1. UV−Vis Data for Azobenzene Derivatives 6a, 7a, and 2a[a]

	trans isomer				*cis* isomer (estimated value)	
compd	λ_{max}	ϵ	λ_{max}	ϵ	λ_{max}	ϵ
azobenzene	447	480 ± 10	318.5	$2.0\ 10^4 \pm 1000$	433	1100 ± 15
6a	444	560 ± 15	323.5	$2.3\ 10^4 \pm 1000$	436	∼1270
7a	435	720 ± 20	348	$2.0\ 10^4 \pm 1000$	441	∼1420
2a	457	485 ± 15	325.5	$2.7\ 10^4 \pm 1000$	436	∼1000

[a] In methyltetrahydrofuran at 293 K.

To compare the efficiencies for photoisomerizations of three azobenzenes (**2a**, **6a**, **7a**), we next examined their photoresponsive properties by kinetic measurements. The quantitative spectral data necessary for calculation of the quantum yields are summarized in Table 1 (cf. SI-2, Figure B). These data show that nitroxide substituents induce some bathochromic shift of the absorption bands. The largest shift of the $\pi\pi^*$ absorption is observed in the case of compound **7a**, containing a long alkyl spacer between the azobenzene and nitroxide moieties. This interesting phenomenon obviously is a result of intramolecular complexation of the azobenzene and nitroxide fragments of the molecule in solution, as it is known that the nitroxide group is inclined to complexation with molecules in almost all classes of organic substances.[11]

The kinetics of reversible photochemical *trans*−*cis* and *cis*−*trans* isomerization is described by the following equation:

$$\frac{dT}{dt} = -I_0\phi_t\frac{A_t}{A_c + A_t}[1 - 10^{-(A_t+A_c)}] + I_0\phi_c\frac{A_c}{A_c + A_t}[1 - 10^{-(A_t+A_c)}] \quad (1)$$

where T is the concentration of the *trans*-isomer in solution, t is the time of light irradiation, I_0 is the intensity of irradiation, ϕ_t and ϕ_c are the quantum yields of the *trans*−*cis* and *cis*−*trans* photoreactions, correspondingly, and A_t and A_c are the absorbances of light by the *trans*- and *cis*-isomers, correspondingly. The thermal *cis*−*trans* isomerization is neglected in eq 1.

Using variable

$$u = \int_0^t \frac{1 - 10^{-(A_t+A_c)}}{A_t + A_c}\,dt$$

eq 1 can be simplified:

$$dT/du = I_0(\phi_c A_c - \phi_t A_t) \quad (2)$$

Taking into account that $A_t = \epsilon_t lT$ and $A_c = \epsilon_c lC$, where C is the concentration of the *cis*-isomer, l is the optical length, and ϵ_t and ϵ_c are the absorption coefficients of the *trans*- and *cis*-isomers, correspondingly, the solution of eq 2 can be presented as

$$\Delta A_\lambda(u) = (\epsilon_c^\lambda - \epsilon_t^\lambda)lT_0\frac{\phi_t\epsilon_t}{\phi_t\epsilon_t + \phi_c\epsilon_c}(1 - e^{-u/\tau}) \quad (3)$$

where ΔA_λ is the change of absorbance of the solution at the wavelength of registration λ, $\epsilon_c^\lambda - \epsilon_t^\lambda$ is the difference in the absorption coefficients at wavelength λ, and

$$\tau = \frac{1}{I_0 l(\phi_t\epsilon_t + \phi_c\epsilon_c)} \quad (4)$$

The value of τ in eq 3 can be determined in the course of kinetic experiments. Figure 2 shows the photoinduced change of the UV−vis spectrum of **6a** in methyltetrahydrofuran in more detail. Typical kinetic curves are presented in Figure 2.

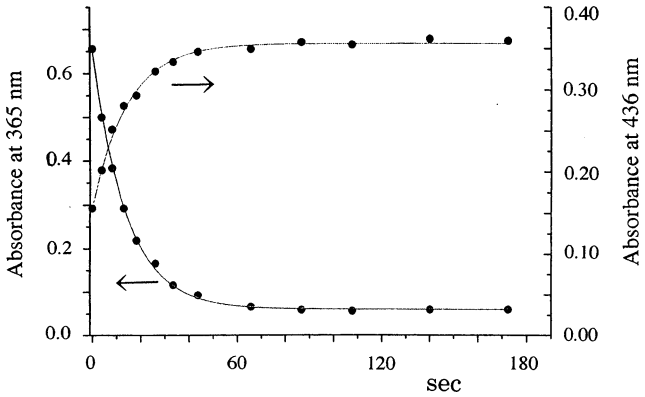

FIGURE 2. Change in the absorbance of the solution of **6a** in methyltetrahydrofuran in the course of irradiation at 365 nm.

One can see from Figure 2 that the absorbance of the solution at 365 nm becomes very small after long irradiation. This observation leads to the following two consequences. The concentration of the *trans*-isomer after long irradiation by light of 365 nm can be neglected, and the absorption coefficient of the *cis*-isomer can be estimated using such a solution. Estimated values for the compounds studied are presented in the SI. On the other hand, the condition $\phi_t\epsilon_t \gg \phi_c\epsilon_c$ allows us to determine of the quantum yield of *trans*−*cis* isomerization using eq 4. The results thus obtained are summarized in Table 2.

Determination of the quantum yields of *cis*−*trans* photoisomerization in the course of irradiation by light of 436 nm is more complicated as there is no wavelength with pure absorbance by one component. As a result the photostationary condition $\phi_c\epsilon_c C^s = \phi_t\epsilon_t T^s$ was used, and the ratio $\phi_c\epsilon_c/\phi_t\epsilon_t$ was determined as

$$\frac{\phi_c\epsilon_c}{\phi_t\epsilon_t} = \frac{T^s}{C^s} \quad (5)$$

Then the quantum yields were calculated using eqs 4 and 5. The results are also presented in the same table. The quantum yields for azobenzene itself were determined as well for comparison. One can see that literature values in different solvents are in good agreement with the values obtained in the present work. The results show that compounds **2a**, **6a**, and **7a** are more photoreactive as compared with azobenzene itself. It

(11) Cf. Buchachenko A. L. *Kompleksy radikalov i molekulyarnogo kisloroda s organicheskimi molekulami (Complexes of Radicals and Molecular Oxygen with Organic Molecules)*; Nauka: Moscow, 1984.

TABLE 2. Quantum Yields of Photoisomerization, ϕ_t and ϕ_c

	irradiation 365 nm		irradiation 436 nm	
compd	*trans* → *cis*	*cis* → *trans*	*trans* → *cis*	*cis* → *trans*
6a	0.16		0.33	0.77
7a	0.30		0.69	0.83
2a	0.055		∼0.29	∼1.0
azobenzene	0.1 (0.11−0.16)[a]	0.26 (0.24−0.31)[a]	0.22 (0.21−0.27)[a]	0.56 (0.46−0.58)[a]

[a] Lit.: Zimmerman G., Chow L.-Y., Paik U.-J. *J. Am. Chem. Soc*., **1956**, *80*, 3528. Bortulus P., Monti S. *J. Phys. Chem*. **1979**, *83*, 648.

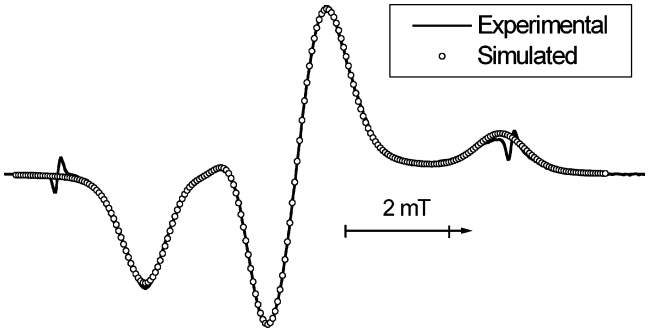

FIGURE 3. EPR spectrum of **6a** in methyltetrahydrofuran at 77 K and the simulated one.

is noteworthy that the largest quantum yields were found for compound **7a** with a long alkyl chain. We presume that this is a result of the influence of the nitroxide group with a long alkyl chain on photophysical processes in the exited state of the molecule.

Magnetic Properties of Azobenzene Derivatives with a Nitroxide. The magnetic data of the azobenzenes in solution are obtained by EPR measurements, and 1:1:1 triplet spectra were always observed in all of the radicals examined irrespective of the difference in substituent, geometry (*trans* and *cis*), and spin source (TEMPO or PROXYL) with similar *g* factors of *ca.* 2.006 and similar coupling constants a_N of around 1.5 mT due to a nitroxide moiety (cf. SI-3, Figure C). A typical EPR spectrum at 77 K in degassed methyltetrahydrofuran and the simulated one for **6a** are shown in Figure 3. To see some difference in the magnetic behavior in solution between the isomer couples, anisotropic parameters were obtained in the course of numerical simulation of the spectrum of **6a** at 77 K, and the data for the three isomer couples including compound **6a** (**2a**/**2b**, **6a**/**6b**, and **7a**/**7b**) show that the spectra of all compounds in both the *trans*- and *cis*-forms coincide within experimental errors (cf. SI-4, Table A).

To verify the intermolecular magnetic interactions of the azobenzene derivatives with a nitroxide group, magnetic measurements of the solid samples were carried out by using a SQUID susceptometer in the temperature range from 2 to 300 K, and the data are summarized in Table 3, in which the data for the *trans*-isomers are given in the upper columns and those for the *cis*-isomers in the lower ones. Thus, an antiferromagnetic interaction being well expressed by the singlet−triplet (ST) model[12] is observed in the radical **2a** with a fairly large exchange interaction of $J/k_B = -47.6$ K. ST behaviors are also revealed in the radicals **8a** and **10a** with a PROXYL substituent, but the J/k_B values (−4.2 K for **8a** and −3.5 K for **10a**) of the radicals are much smaller than that found in **2a**. On the other hand,

TABLE 3. Solid-State Magnetic Data of Azobenzene Derivatives with Nitroxide

compd	magnetic interaction	C[a]/emu K mol^{-1}	Θ[b]/K	(J/k_B)/K
2a	antiferromagnetic			−47.6[c] (100)
6a	antiferromagnetic			−1.89[d] (91)
7a	ferromagnetic	0.38 (100)	0.09	
8a	antiferromagnetic			−4.2[c] (83)
9a	antiferromagnetic	0.36 (95)	−12	
10a	antiferromagnetic			−3.5[c] (92)
11a	ferromagnetic			0.16[d] (84)
12a	antiferromagnetic	0.35 (93)	−0.22	
2b	ferromagnetic	0.38 (100)	0.11	
6b	ferromagnetic	0.38 (100)	0.32	
7b	antiferromagnetic			−36.7[c] (64)
8b	antiferromagnetic			−7.7[c] (76)

[a] Curie constant. Numbers in parentheses denote the estimated spin concentrations, by using a theoretical Curie constant of 0.375 emu K mol^{-1}. [b] Weiss temperature. [c] Exchange interactions obtained by fitting with the singlet−triplet model. [d] Exchange interactions obtained by fitting with the 1-D Heisenberg model. Numbers in parentheses denote estimated spin concentrations.

antiferromagnetic interactions being based on the Curie−Weiss (CW) model are observed in the *trans*-azobenzenes **9a** and **12a**, while weak ferromagnetic interaction of CW behavior is found for the *trans*-azobenzene **7a**. The magnetic behavior of the radical **6a** and 4-nitro-substituted azobenzene with TEMPO (**11a**) can be well analyzed by the one-dimensional Heisenberg model[13] with an antiferromagnetic exchange interaction of $J/k_B = -1.89$ K for **6a** and a small ferromagnetic one of $J/k_B = 0.16$ K for **11a** (vide infra; cf. SI-5, Figure D, and SI-6, Figure E).

While the existence of a fairly strong antiferromagnetic interaction based on the ST model is clarified in the *trans*-isomer of ester derivative **2a**, a weak ferromagnetic interaction with CW behavior is observed in the corresponding *cis*-isomer **2b** as shown in Figure 4, indicating the occurrence of an apparent change in the intermolecular magnetic interactions between the photoisomer couple originating possibly from the change in the molecular/crystal structures.

Although weak intermolecular magnetic interactions are preserved between the photoisomer couple **6a** and **6b**, apparent antiferromagnetic interaction observed in the spins of **6a** is changed to a ferromagnetic one in those of **6b**. As regards the photoisomer couple **8a** and **8b** with a PROXYL group, the magnitudes of the exchange interactions (J/k_B values) are apparently altered by the structural change as indicated in Table 3. Namely, the ST behavior with a weak antiferromagnetic

(12) Bleaney, B., Bowers, K. D. *Proc. R. Soc. London, Ser. A* **1952**, *214*, 451.

(13) Bonner J. C., Fisher, M. E. *Phys. Rev. A* **1964**, *135*, 640. In fact, the radical molecules in the crystal are found to consist of two kinds of chain structures: one gives rise to ferromagnetic interaction and the other to antiferromagnetic interaction, and the best fit to the experimental data is obtained in the present case by considering overwhelmingly the latter one with the 1-D Heisenberg model.

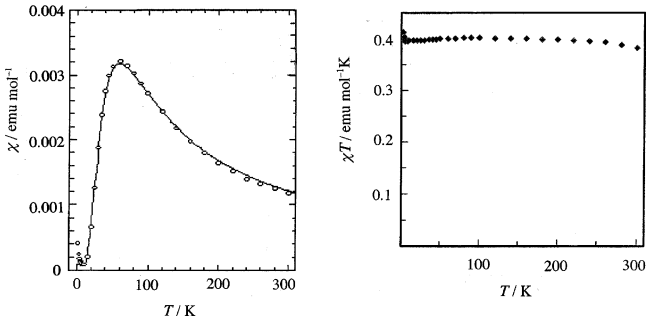

FIGURE 4. Magnetic suscptibility data of *trans*-isomer **2a** (left, $\chi-T$ data) and the corresponding *cis*-isomer **2b** (right, $\chi T-T$ data). The solid line in the left panel is the theoretical curve fitted by the ST model (see the text).

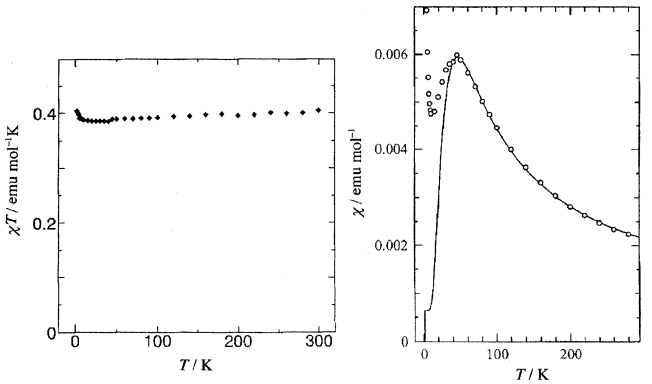

FIGURE 5. Magnetic data of *trans*-isomer **7a** (left, $\chi T-T$ data) and the corresponding *cis*-isomer **7b** (right, $\chi-T$ data). The solid line in the right panel is the theoretical curve fitted by the ST model (see the text).

interaction ($J/k_B = -4.2$ K) in the *trans*-isomer **8a** is changed to ST behavior with an antiferromagnetic interaction of an almost 2 times larger value ($J/k_B = -7.7$ K) in the *cis*-isomer **8b**. A more impressive change in the intermolecular interactions is found in the photoisomer couple **7a** and **7b** (Figure 5). That is, the original CW behavior with a weak ferromagnetic interaction ($\Theta = 0.09$ K) is changed to ST behavior with a fairly strong antiferromagnetic interaction with a J/k_B value of *ca.* -37 K, suggesting closer contact of the spin centers evoked by the structural change.[14] Thus, a series of photoresponsive spin systems showing different changes in their intermolecular magnetic interactions could successfully be constructed in these cases.

Interestingly, a heat-responsive magnetic property has also been disclosed in the *cis*-isomer **7b**. While no appreciable change could be discerned in the *trans*-isomer **7a** during the heating process to 400 K (mp ca. 380 K) and successive cooling process (Figure 6, left), an apparent change was observed in the *cis*-isomer **7b** during the processes, when heated over its melting point (ca. 310 K) as shown in Figure 6 (right). Namely, an appreciable increase of the χ values in the lower temperature region together with a decrease of the exchange interaction to $J/k_B = -14$ K from the original J/k_B value of ca. -37 K is observed during the cooling process in the isomer **7b**. Although the reason why the different magnetic behaviors are observed

(14) The discrepancy between the experimental and theoretical curves in the low-temperature region is considered to be due to the presence of a small amount of paramagnetic impurities and/or defects, and they are neglected in this case.

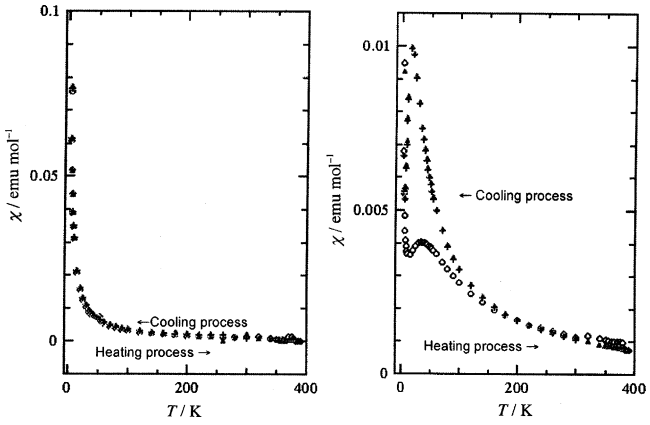

FIGURE 6. Magnetic data for *trans*-isomer **7a** (left) and *cis*-isomer **7b** (right) between 2 and 400 K and during the heating (open square) and cooling (closed triangle) processes. The reheating data (plus signs) are also indicated with almost no difference from the cooling data for both compounds.

in the heating and cooling processes is not clarified yet, and although the occurrence of a change in the molecular configuration of the *trans*-isomer **7a** cannot be considered from the magnetic data, a change of the molecular pacing is presumed to happen by thermal phase transition to give different J/k_B and χ values, respectively. Such a heat-responsive property is considered to be due partially to the existence of a long alkoxy group in the radical **7b** as seen in the previous examples **II** and **III**, although this is not the case for the *trans*-isomer **7a**. Thus, the photoisomer couple **7a** and **7b** is regarded as a kind of photoresponsive as well as heat-responsive spin system.

Molecular/Crystal Structures of *trans*-Azobenzene Derivatives with a Nitroxide (2a, 6a, 7a, 8a, and 11a). A single crystal suitable for X-ray analysis was obtained for the radical **2a** by recrystallization from hexane/diethyl ether, and its structure with a *trans*-configuration of the azobenzene moiety is apparent from X-ray analysis (Figure 7). The oxygen−oxygen distance of the neighboring spin centers amounts about to 3.5 Å, which is relevant to the behavior being based on the ST model observed in the radical with a fairly strong antiferromagnetic interaction of $J/k_B = -47.6$ K.[9,12] A single crystal could also be obtained by recrystallization of the ester isomer **6a** from hexane/diethyl ether, and the crystal structure is shown in Figure 8. In this crystal, the molecules are found to be formed of interconnecting chains, and its magnetic property is regarded to be predominantly governed by antiferromagnetic chains, being well analyzed by the 1-D Heisenberg model, with $J/k_B = -1.89$ K (vide supra).[13]

The crystal structure of the TEMPO derivative **7a** is shown in Figure 9, and two molecules are depicted in the figure. Thus, the molecules have long alkoxy chains attached to *trans*-azobenzene cores and TEMPO groups at their ends. The molecules form a sheetlike structure on the *bc* plane, and the nearest oxygen−oxygen distance of the neighboring spin centers is estimated to be ca. 6 Å, which is fairly far apart for giving a strong intermolecular magnetic interaction and is relevant to the observed very weak magnetic interaction in this radical.

In Figure 10, the crystal structure of the corresponding PROXYL derivative **8a** is indicated, and two molecules are depicted in this case as well. Thus, the molecules also have long alkoxy chains attached to *trans*-azobenzene cores and PROXYL groups at their ends, and the O−O distance of the

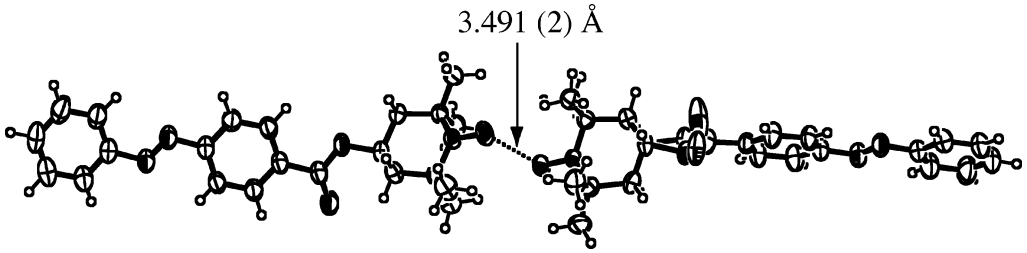

FIGURE 7. Crystal structure of **2a** indicating oxygen−oxygen distances of the spin centers and the spins on them.

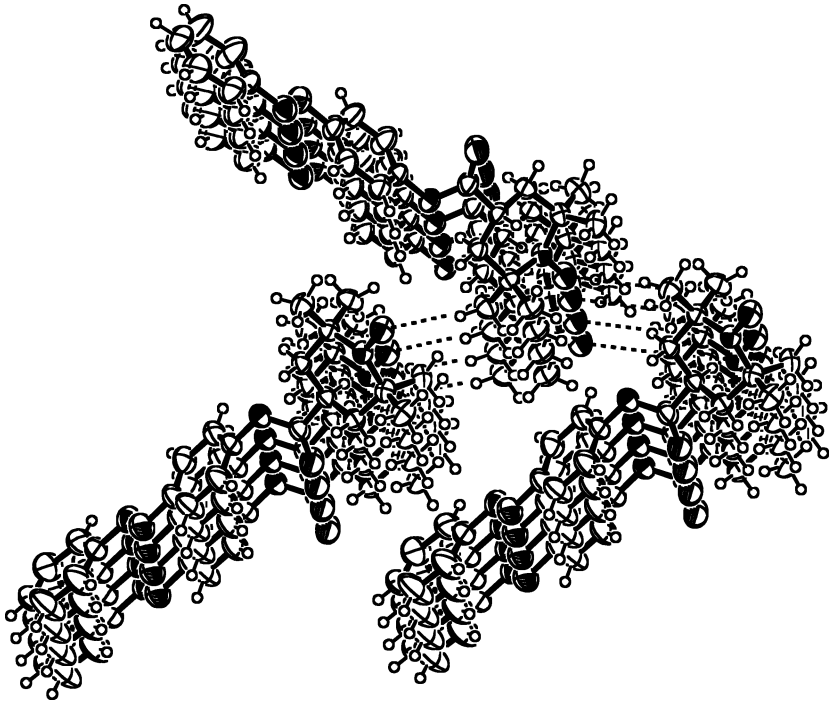

FIGURE 8. Crystal structure of **6a** indicating 1-D magnetic chains with dotted lines.

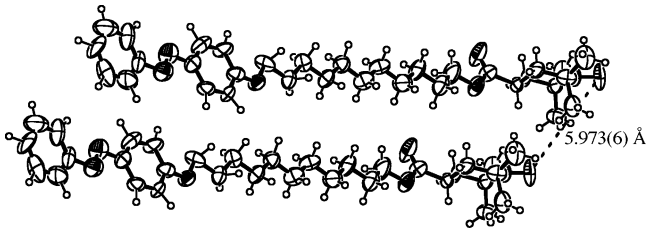

FIGURE 9. Crystal structure of **7a** (two molecules are depicted) indicating oxygen−oxygen distances of the spin centers.

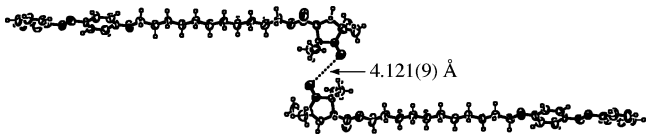

FIGURE 10. Crystal structure of **8a** (two molecules are depicted) indicating oxygen−oxygen distances of the spin centers.

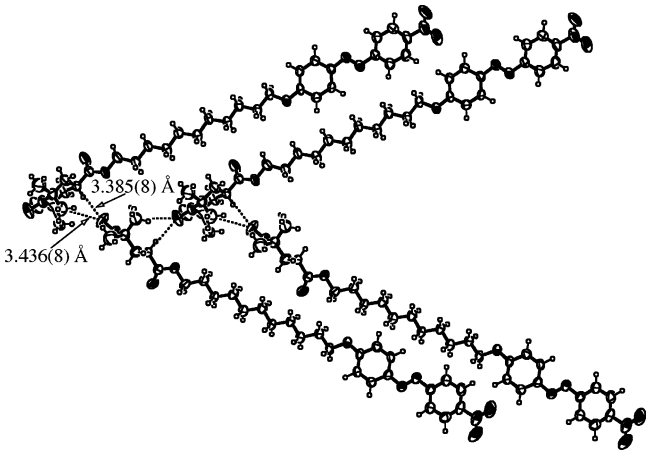

FIGURE 11. Crystal structure of **11a** (four molecules are depicted) indicating short contacts between the next neighbor molecules.

spin centers between the molecules amounts to ca. 4.1 Å, which is considered to be responsible for the ST behavior with a weak antiferromagnetic interaction.

The crystal structure of *p*-nitroazobenzene derivative **11a** is shown in Figure 11, and there are a couple of short contacts between the oxygen atom of a TEMPO group and the neighboring molecule, forming on the whole a 1-D chain structure and thus reflecting the magnetic behavior of the 1-D Heisenberg model observed in the derivative **11a** (see Table 3).

However, any attempt to prepare a single crystal of the corresponding *cis*-isomers has so far been unsuccessful probably

because of the unstable nature of the isomers, particularly in solution.

Conclusions

We prepared a series of *trans*-azobenzene derivatives with nitroxide substituents and investigated their photoisomerization reactions as well as magnetic properties. The crystal structures of some of the derivatives could be clarified, and their structure/magnetic property relations were investigated. Among the *trans*-azobenzenes prepared, the unsubstututed derivatives at the *para*-position (**2a**, **6a**, **7a**, **8a**) were found to undergo photoisomerizations by irradiation to give the corresponding *cis*-isomers (**2b**, **6b**, **7b**, **8b**), being isolated as relatively stable solid materials. The respective changes of the intermolecular magnetic interactions were apparently observed by the structural changes for all of the photochromic couples, and a kind of multifunctionality with photoresponsive as well as heat-responsive properties was disclosed in the photoisomer couple **7a**/**7b**.

Experimental Section

Materials. 4-Carboxy- and 4-hydroxy-TEMPO radicals as well as 4-carboxy-, 4-hydroxy-, and 4-nitro-4′-hydroxyazobenzenes used as building blocks in this study are commercially available. 4-(Dimethylamino)-4′-hydroxyazobenzene[15] was prepare by the coupling of diazonium salt from 4-aminophenol with *N*,*N*-dimethyaniline.

Instrumentation. Melting points of the solid samples are uncorrected. The UV−vis spectra were measured in dichloromethane or methyltetrahydrofuran solution at ambient temerature. The FAB-MS spectral data were obtained by using *m*-nitrobenzyl alcohol as the matrix and the appropriate polyethylene glycol sample as the internal standard. The *g* values of the EPR data were determined using Mn^{2+}/MgO maker as an internal standard. Susceptibility measurements were carried out using ca. 10 mg for each powdered sample in the usual way.[16] Photolysis experiments for kinetic studies were performed with a mercury high-pressure lamp (500 W). Light of the required wavelength was isolated using standard glass filters. The intensity of incident light was determined by ferrioxalate actinometry[17] (for light of 365 nm) and Reinekate salt actinometry[18] (for light of 436 nm). These experiments were performed with samples degassed by a repeated procedure of freezing−pumping−melting.

Preparation of TEMPO-Substituted Azobenzenes 2a and 6a. To a stirred mixture of 4-carboxyazobenzene (**1**) (0.26 g, 1.2 mmol) and 4-hydroxy-TEMPO (0.20 g, 1.2 mmol) in dichloromethane (30 mL) were added DCC (0.29 g, 1.4 mmol) and DMAP (0.17 g, 1.4 mmol) at ambient temperature. After being stirred for 1 d and after the precipitated urea was filtered off, the reaction mixture was concentrated in vacuo to give an orange solid, which then was purified by column chromatography on silica gel with the solvent system of hexane and diethyl ether and recrystallized from the same system. The *trans*-azobenzene **2a** was obtained as orange plates (0.29 g, 66%). Mp: 127−130 °C. EPR data: see the SI. Anal. Calcd for $C_{22}H_{26}N_3O_3$: C, 69.45; H, 6.89; N, 11.04. Found: C, 69.81; H, 6.95; N, 11.22. In a similar manner, the isomeric azobenzene **6a** was prepared by using 4-hydroxyazobenzene (**3**) and 4-carboxy-TEMPO as starting materials and was obtained as yellow needles by recrystallization from *n*-hexane and diethyl ether. Mp: 151−154 °C. EPR data: see the SI. Anal. Calcd for $C_{22}H_{26}N_3O_3$: C, 69.45; H, 6.89; N, 11.04. Found: C, 69.23; H, 6.84; N, 11.08.

Preparation of Nitroxide-Substituted *trans*-Azobenzenes 7a−12a. The preparation of a TEMPO-substituted derivative (**7a**) is described as an example: A stirred solution of 4-hydroxyazobenzene (0.20 g, 1.0 mmol), (bromoundecanoxy)carbonyl-TEMPO[9] (0.44 g, 1.0 mmol), and potassium carbonate (0.42 g, 3.0 mmol) in a mixed solvent of DMF/THF (3:1, 40 mL) was heated to reflux, and heating was continued for 20 h. After being cooled to room temperature, the reaction mixture was filtered and washed with THF, and the filtrate was concentrated in vacuo to give a brown-yellow solid, which was purified by column chromatography on silica gel by using the solvent system of benzene and diethyl ether and then recrystallized from a mixed solvent of hexane and methanol. The derivative **7a** was obtained as yellow needles (0.40 mg, 71%). Mp: 106−108 °C. EPR data: see the SI. Anal. Calcd for $C_{33}H_{49}N_3O_4$: C, 71.83; H, 8.95; N, 7.62. Found: C, 71.64; H, 8.77; N, 7.83. In a similar manner, the derivatives **8a** ((bromoundecanoxy)carbonyl-PROXYL[9] is used in place of (bromoundecanoxy)-carbonyl-TEMPO), **9a** (4-(dimethylamino)-4′-hydroxyazobenzene is used in place of 4-hydroxyazobenzene), **10a**, **11a** (4-nitro-4′-hydroxyazobenzene is used in place of 4-hydroxyazobenzene), and **12a** were prepared in 72%, 16%, 41%, 30%, and 68% yields, respectively, and their data are as follows. (**8a**) Yellow needles. Mp: 133−136 °C. EPR (benzene): three lines, $g = 2.006$, $a_N = 1.42$ mT. Anal. Calcd for $C_{32}H_{47}N_3O_4$: C, 71.47; H, 8.81; N, 7.82. Found: C, 72.20; H, 8.94; N, 7.70. (**9a**) Yellow powdery solid. Mp: 122−126 °C. EPR (benzene): three lines, $g = 2.006$, $a_N = 1.54$ mT. Anal. Calcd for $C_{35}H_{53}N_4O_4$: C, 70.79; H, 9.00; N, 9.44. Found: C, 70.77; H, 9.26; N, 9.48. (**10a**) Yellow solid. Mp: 117−122 °C. EPR (benzene): three lines, $g = 2.006$, $a_N = 1.44$ mT. FAB-HRMS (*m/z*): calcd for $C_{34}H_{52}N_4O_4$ (M + 1) 580.3989, found 580.4046. (**11a**) Orange-yellow needles. Mp: 105−108 °C. EPR (benzene): three lines, $g = 2.006$, $a_N = 1.54$ mT. FAB-HRMS (*m/z*): calcd for $C_{33}H_{47}N_4O_6$ 595.3496, found 595.3522. (**12a**) Orange-yellow solid. Mp: 96−100 °C. EPR (benzene): three lines, $g = 2.006$, $a_N = 1.44$ mT. FAB-HRMS (*m/z*): calcd for $C_{32}H_{45}N_4O_6$ 581.3339, found 581.3367.

Preparation of Nitroxide-Substituted *cis*-Azobenzenes 2b, 6b, 7b, and 8b by Photochemical Isomerization. The preparation of a TEMPO-substituted derivative (**6b**) is described as an example: A dichloromethane solution (20 mL) of *trans*-azobenzene derivative **6a** (0.10 g, 0.26 mmol) was irradiated by a lamp with light of 365 nm for 6 h. The solvent was then evaporated carefully under reduced pressure in the dark to avoid *cis* to *trans* isomerization by light, and the resulting solid was purified in the dark by short-column chromatography on silica gel with the solvent system of *n*-hexane and diethyl ether. After the elution of a small amount of less polar *trans*-isomer **6a**, relatively polar *cis*-isomer **6b** could be isolated as an orange powdery solid (77 mg, 77%). Mp: 110−113 °C. EPR data: see the SI; FAB-HRMS (*m/z*): calcd for $C_{22}H_{26}N_3O_3$ 380.1974, found 380.1977. In a similar manner, the derivatives **2b**, **7b**, and **8b** were prepared in 38%, 40%, and 50% yield, respectively, and their data are as follows. (**2b**) Mp: 134−135 °C. EPR data: see the SI. FAB-HRMS (*m/z*): calcd for $C_{22}H_{26}N_3O_3$ 380.1974, found 380.1962. (**7b**) Mp: 34−37 °C. EPR data: see the SI. FAB-HRMS (*m/z*): calcd for $C_{33}H_{49}N_3O_4$ (M + H) 551.3723, found 551.3698. (**8b**) Mp: 123−125 °C. EPR (benzene) three lines, $g = 2.006$, $a_N = 1.44$ mT. FAB-HRMS (*m/z*): calcd for $C_{32}H_{46}N_3O_4$ 536.3488, found 536.3438.

Acknowledgment. This work was supported by a Grant-in-Aid for Scientific Research (No. 13440213) from the Japan Society for the Promotion of Science (JSPS) and a special grant from the University of Hyogo and the Russian Foundation for Base Reserch (06-03-32231).

(15) Burawoy, A.; Salem, A. G.; Thompson, A. R. *J. Chem. Soc.* **1952**, 4793.
(16) Nakatsuji, S.; Takai, A.; Nishikawa, K.; Morimoto, Y.; Yasuoka, N.; Suzuki, K.; Enoki, T.; Anzai, H. *J. Mater. Chem.* **1999**, *9*, 1747.
(17) Kurien K. C. *J. Chem. Soc. B* **1971**, 2081.
(18) Wegner, E. E.; Adamson, A. W. *J. Am. Chem. Soc.* **1966**, *88*, 394.

Supporting Information Available: Figures showing the absorption change of **6a** by irradiation (SI-1, Figure A), the absorption spectra of **2a**, **6a**, and **7a** (SI-2, Figure B), the EPR spectra of **6a** (SI-3, Figure C), and the magnetic susceptibility data for **6a** and **11a** (SI-5, Figure D, and SI-6, Figure E), a table of EPR data for three isomer couples (**2a**/**2b**, **6a**/**6b**, and **7a**/**7b**) (SI-4, Table A), a summary of the X-ray structure determination (SI-7), and CIF files of the crystallographic data (tables of crystal data, bond lengths and angles, atomic coordinates, and anisotropic thermal parameters) for **2a**, **6a**, **7a**, **8a**, and **11a**. This material is available free of charge via the Internet at http://pubs.acs.org.

JO062266F